Development of a Deep Neural Network (DNN) Model for Feature Selection from Satellite Images

Soma Mitra[1], Debkumar Chowdhury[2], Mauparna Nandan[3], Kajori Parial[4]*, Saikat Basu[5]

[1] Computational Science, Brainware University, 398, Ramkrishnapur Road, Near Jagadighata Market, Barasat - 700125, West Bengal, India.

[2] Computer Science and Engineering, University Of Engineering & Management, University Area, Plot No. III, B/5, New Town Rd, Action Area III, New Town - 700160, West Bengal, India.

[3] Department of Computer Applications, Techno India Main, Sector V , Saltlake - 700091, West Bengal, India.

[4] Department of Geoinformatics and Spatial Sciences, Maulana Abul Kalam Azad University of Technology, BF Block, Sector 1, Bidhannagar, Kolkata - 700064, West Bengal, India.

[5] Computer Science and Engineering, Maulana Abul Kalam Azad University of Technology, BF Block, Sector 1, Bidhannagar, Kolkata -700064, West Bengal, India.

*Corresponding author(s). E-mail(s): kajorigis@gmail.com; saikatbasu@gmail.com
Contributing authors: somadocuments@gmail.com; debkumar.cse@gmail.com; mauparna2011@gmail.com;

The paper is a non-peer reviewed preprint submitted to EarthArXiv.

Twitter handle @beas4evr

Development of a Deep Neural Network (DNN) Model for Feature Selection from Satellite Images

Soma Mitra[1], Debkumar Chowdhury[2], Mauparna Nandan[3], Kajori Parial[4*], Saikat Basu[4†]

[1]Computational Science, Brainware University, 398, Ramkrishnapur Rd, Near Jagadighata Market, Barasat, 700125, West Bengal, India.
[2] Computer Science and Engineering, University Of Engineering & Management, University Area, Plot No. III, B/5, New Town Rd, Action Area III, New Town, 700160, West Bengal, India.
[3] Department of Computer Applications, Techno India Main, Saltlake, Sector V , saltlake, 700091, West Bengal, India.
[4*]Computer Science and Engineering, Maulana Abul Kalam Azad University of Technology, BF Block, Sector 1, Bidhannagar, Kolkata, 700064, West Bengal, India.

*Corresponding author(s). E-mail(s): kajorigis@gmail.com;
Contributing authors: somadocuments@gmail.com; debkumar.cse@gmail.com; mauparna2011@gmail.com; saikatbasu@gmail.com;
†S. M. has conceived and designed the research. S. M. has also prepared the draft manuscript. S.M., D.C. and M.N. has executed the research including development of DNN architecture, RF and XGBoost modelling. K. P. has guided and finalised the manuscript for submission. S.B. has coordinated the research and manuscript preparation.

Abstract

Advances in space-based observation, using remotely sensed data, has proved to be an important tool to monitor the globe, including the areas inaccessible to humans. The Sundarban deltaic region, witnessing the confluence of vast expanses of tropical mangrove forests, tidal rivers, and estuaries, is one such area. Considered as one of the richest biodiversity hotspot zones on earth, home to a large spectrum of biodiversity (flora and fauna), including endangered or threatened

species, this forest plays a critical role in land reclamation, coastal habitat protection, and local socioeconomics. However, the forests have been experiencing changes due to climatic forces and anthropogenic activities. Monitoring these changes is crucial for adopting precise management practices. In this work Landsat 8 images were used to identify the land use and land cover in the Sundarbans. For classification, a new deep Neural Network (DNN) model is proposed. A comparative analysis of overall accuracy (OA) of the proposed DNN model with two popular Machine Learning (ML) models, Random Forest (RF) and XGBoost showed 98.9% 97.0% and 98.1% OA respectively. Additive exPlanations (SHAP) were used for each model to obtain important features. It was observed that NIR, SWIR1, Blue, and EVI were the most important features. The proposed DNN model outperformed the RF and XGBoost models with these four important features, achieving 98.5% accuracy. On comparison, it was concluded that deep learning techniques are more effective in feature selection from remote sensing images.

Keywords: XGBoost, Random Forest, Explainable AI, DNN, Sundarbans

1 Introduction

In recent decades, the images from Earth observation satellites have been found instrumental in providing a synoptic view of the Earth's surface. These images are also used extensively for mapping, analyzing and monitoring the changing dynamics of the earth's surface, almost in real-time in some instances, facilitating decision-makers and managers to act appropriately. Driven by technological and computational advancements, satellite data acquisition has become faster, more versatile, and voluminous compared to their ancestors. The challenge lies in extracting maximum information and generating insight from these images of high spatial, temporal, and spectral resolutions, within a very short time. Acknowledging the human limitations, the machines are trained with real and labelled data to identify patterns, objects or instances available in each image scene. Based on the training, Machine Learning (ML) models are developed. This process of training machines using real and labelled data and generating models is commonly called Machine Learning (ML). Once the desired accuracy is attained through testing and validation, the model is employed to extract information from unknown data. The accuracy of the test results determines the final output model for a specific application.

Broadly, ML is used for classification, image segmentation, and object recognition. Pixel-level classification techniques were considered the most effective when satellite images were of low resolution. As the resolution of the sensors increased, image patches or sub-images of even larger size along with the context information - called features, were identified from the images. This type of classification is known as feature-based remote sensing scene classification/recognition. They are extensively used for land cover and land use classification tasks [1, 2]. These algorithms use labelled training data to discover patterns and relationships to assign class labels to unlabelled data automatically. For classification, many ML approaches such as random forests (RFs),

support vector machines (SVMs), and artificial neural networks (ANNs) have been used [3–5].

In image segmentation, an image is divided into several sections based on common patterns, thus helping in the extraction of different regions of interest [6]. By learning from training examples to identify object borders or areas, ML algorithms can handle this task successfully [7]. [8] adopts cutting-edge DCNN computer vision frameworks for semantic segmentation of MSI imaging. Generated synthetic MSI was replaced with actual MSI to initialize a DCNN framework in order to overcome label scarcity for MSI data. The framework was evaluated with a brand-new RIT-18 dataset.

Object identification aims to detect and identify specific objects or features within remote sensing imagery [9]. ML algorithms can be trained to recognize and classify objects of interest, such as buildings, roads, vegetation, and water bodies. [10] used a Mask Region-based Convolutional Neural Network (Mask-RCNN) for building extraction from satellite data. [11] The method initially collected specific building multi-feature data from multitemporal high-resolution pictures, including texture, indices, spectral, and shape. Then, using the multi-feature data, a planned LSTM network architecture with an ideal unit number is trained to extract buildings at the pixel level. Experiments showed that the suggested strategy outperforms existing deep learning-based building extraction techniques.

In this paper, our first objective is to develop a deep neural network (DNN) model for feature selection from satellite images. Two established ML models namely Random Forest (RF) and XGBoost algorithms are also used on the same data to compare the efficiency of the DNN model over them. The Sundarbans, India is selected as the study area.

The Sundarbans, spanning across the coasts of India and Bangladesh, located in the delta of the Ganges, Meghna, and Brahmaputra rivers, are the largest stretch of mangrove forest in the world. Mangroves are woody plants that grow along coastal regions and are known for their ability to withstand high salt levels. They create highly productive inter-tidal ecosystems and are crucial for the coastal environment, including fisheries. It is a well-accepted fact that the Sundarban is a critical ecosystem, providing numerous ecological, social, and economic benefits to local communities and the region. However, in a study by [12] it was reported that the Sundarban is facing significant threats due to anthropogenic activities such as deforestation, land-use change, pollution, and natural disasters like cyclones and sea-level rise. This highlighted the need for the conservation of the forest as a global priority.

In another study, Dutta and Deb[13] used satellite images to calculate the extent of the land cover changes in the region for a period of 26 years from 1984 to 2010. They identified the factors contributing to these changes, such as natural disasters, climate change, and human activities. Since the turn of the millennium in 2000, much research has been published on the Sundarban region using different satellite images.

Research papers [14, 15] used statistical indices like the Forest Canopy Density (FCD) and Normalized Difference Vegetation Index (NDVI) using available band data and analyzed the land cover change. However, the statistical indices have some inherent demerits. NDVI and FCD are sensitive to the types of vegetation present in the forest cover, which can affect their accuracy. Some vegetation types may not be well-suited

to NDVI or FCD analysis, resulting in errors or biases.
Most recent works incorporate ML and DL models for land cover classification in the Sundarban region. The unsupervised classification ISODATA and the Continuous Change Detection and Classification (CCDC) are used in [16] and [17], respectively, with high-level land cover classification accuracy. The former paper achieved 89.89% accuracy, whereas the latter achieved 94.5% overall accuracy. Sardar et al.[18] aimed to understand the landscape dynamics of the Sundarban area using a Multi-Layer Perceptron (MLP) Markov Chain model. The MLP was developed using the land cover maps and landscape metrics for the years 1990, 2000, and 2010. The model was used to predict future land cover changes in the study area. Using ML algorithms, Nasrin et al. [19] assessed the impact of the super cyclone Amphan that hit the Sundarban in May 2020. The study utilized two remote sensing images to extract and analyze the pre- and post-cyclone conditions of the area. It used two ML algorithms, namely artificial neural networks (ANN) and RF, to model the impact of the cyclone on different land cover classes in this region. The RF model was used to classify land cover types and estimate the changes in each class before and after the cyclone. The ANN algorithm was used to estimate the damage level in each land cover class based on the extent of change observed in the RF classification. Finally, the study analyzed the spatial distribution of the impacted areas and provided recommendations for restoration and management of the affected areas. Khan et al. [20] tried a methodology that involved the acquisition of satellite images from Landsat 5 and 8 sensors for three different periods (1990, 2000, and 2015). It used supervised classification algorithms, such as the maximum likelihood algorithm, decision tree algorithm, and random forest algorithm, to classify land cover types. 1 Table 1 provides a summary of the literature discussed here.
A thorough study of these works reveals two trends. One of the trends uses the statistical analysis of the land cover to identify the long-term changes that happened, and another trend adopts ML and DL methods to classify the pixels of the satellite images in order to analyze the mangrove extent over a period. It is noteworthy that the individual pixel values of an image are typically derived from different satellite bands such as visible, near-infrared, and thermal infrared. The values of each pixel can be used to identify different features on the ground, such as water, vegetation, and built-up areas. However, increasing the number of bands in satellite data can increase the complexity of ML models used for classification or regression tasks. Hence, by identifying and selecting the most relevant bands, the dimensions of the data can be reduced significantly. In this way, the danger of overfitting can be reduced.

So, it could be inferred that there is scope for implementing sophisticated ML models in this area, which could provide better efficiency than the discussed research papers and find the important spectral bands that contribute more than the other features for land cover classification.
Thus in this work, our second objective is to choose the relevant features using Explainable Artificial Intelligence (XAI) techniques, such as SHapley Additive ex-Planations (SHAP) technique for land cover classification in the Sundarbans. Effective selection of the most important features from the XAI (Lundberg and Lee 2017) model will lead to a significant dimensionality reduction of the data set,

Table 1: Summary of the Discussed Papers

Reference	Findings	Remarks
[12]	These findings highlight mangrove forests' global distribution and extent and emphasize the need for improved databases and conservation efforts to protect these valuable ecosystems.	Overall, the research paper provides valuable insights into the status and distribution of mangrove forests but lacks a discussion on reliance on satellite data, which may have inherent limitations in capturing certain characteristics of mangrove forests.
[13]	The study highlights the challenges and changes in the Sunderbans mangrove ecosystem, emphasizing the need for proper remedies and sustainable management strategies to address the multidimensional threats and protect this valuable natural resource.	ISODATA incorporated in ERDAS IMAGINE software is used for classification. Lack of comparative analysis of ML and ANN models in land cover classification.
[14],[15]	Illustrates the importance of statistical and vegetation indices for land cover classification.	As every index has its own limitations, they could be used as a feature to classify the land cover in conjunction with the spectral bands.
[18]	The study examines land cover dynamics over three decades (1998-2018) using multi-temporal Landsat images. The findings indicate minimal overall change in the mangrove forest area but significant changes in open and dense mangrove areas to expand human habitat and aquaculture.	The study focuses on the dynamics of land cover changes and the expansion of human habitat and aquaculture; it does not thoroughly investigate the ecological consequences of these changes on the biodiversity and overall health of the different species of the mangrove forest.
[19]	The findings of the study on the impact of Super Cyclone Amphan on land use land cover (LULC) in the Sundarban Biosphere Reserve (SBR) reveal significant changes in the region. Using ML algorithms, the researchers constructed LULC maps before and after the cyclone, with Support Vector Machine (SVM) yielding the highest accuracy.	The study employed ML algorithms for land cover classification; there is an opportunity to investigate and compare the performance of other state-of-the-art algorithms or hybrid approaches. Additionally, incorporating more sophisticated image processing techniques, such as object-based image analysis or deep learning methods, could potentially improve the accuracy and efficiency of land cover mapping.
[20]	This paper applied ML techniques to analyze remote sensing data from the Sundarbans mangrove forest, achieving overall accuracy rates ranging from 75% to 80% for land cover classification in 2001, 2011, and 2021. The study revealed a 0.2% decline in the forest's land cover over the past two decades, primarily due to human settlements, deforestation, natural calamities, and increased water salinity	20 Years of satellite data should be tested with other sophisticated ML models to improve accuracy and better insight of the present and past scenarios of the land cover changes. Additionally, integrating higher-resolution satellite imagery or aerial drones could provide more detailed and up-to-date information to understand land cover changes better.

reduction in the complexity of the models as well as, it will also significantly enhance

the transparency and interpretability of the DNN model., using Explainable Artificial Intelligence (XAI) techniques, such as SHapley Additive ex-Planations (SHAP) values are calculated.

2 Data

Data points for the study were collected from Landsat 8 Level 2 Image covering the parts of Sundarbans (Path 138 and Row 45) across the geographical extent of 21°53′N to 22°03′N and 88°46′E to 89°29′E. Data points were collected under five different land cover classes, namely - water, mangroves, sandbanks, mudflats, and others, using Google Earth Engine (GEE). Apart from the six bands of the Landsat image, three different vegetation indices were also calculated and considered for classification for better vegetation identification. Thus each collected data point was represented by nine bands, henceforth called features, six bands (Blue, SWIR1, SWIR2, NIR, Red, Green) of Landsat image and the three vegetation indices bands - NDWI, GNDVI, and EVI. Surface reflectance values of the image bands and the pixel value of respective indices bands for each data point were combined into one CSV file. Table 2 describes the data point distribution used in the present study. The data were then normalized using the z-score normalization method for better results [21]. The Z-score normalization equation is given in Equation 1.

$$Normalized\,Value = \frac{X - \mu}{\sigma} \tag{1}$$

where X is the current pixel value, σ is the standard deviation, and μ is the mean.

Table 2: Data Points Distribution In Different Classes

	Water	**Mangrove**	**SandBank**	**MudFlat**	**Other**
No of Data Points	14,343	3,845	1,218	3,450	9,214

3 Methodology

Figure 2 depicts the approach for identifying relevant variables that influence the classification model. After generating the data set, three vegetation indices were calculated, considering more features for classification, thus boosting the classification accuracy. The following section describes the indices used in this study followed by a description of the DNN model developed for the study. The two ML models namely Random Forest and XGBoost are also discussed briefly.

3.1 Vegetation and Water Indices

The purpose of indices is to optimize the ability to detect vegetation and water bodies while reducing the impact of factors that may interfere with accurate readings, such as soil background reflectance, atmospheric effects, and directional influences [22, 23].

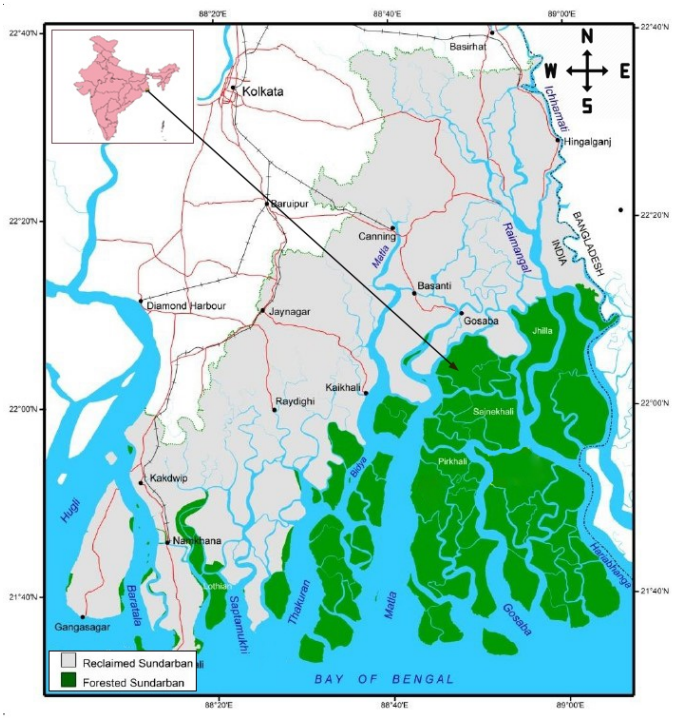

Fig. 1: Map Of the Sundarban Region

The indices used in this study are briefly discussed below.

Enhanced Vegetation Index (EVI) quantifies vegetation greenness by correcting canopy background noise and atmospheric conditions.

$$EVI = 2.50 * ((NIR - RED)/(NIR + 6.00 * RED - 7.50 * BLUE + 1)) \quad (2)$$

The constant values in the formula have been empirically determined to optimize the vegetation signal. EVI values typically range from -1 to 1, with higher values indicating denser and healthier vegetation.

Green Normalized Difference Vegetation Index (GNDVI) measurement involves capturing the green spectrum, which provides an indication of the vegetation's photosynthetic activity. This method is particularly effective at detecting chlorophyll concentration and is considered more responsive than other indices.

$$GNDVI = \frac{(NIR - GREEN)}{(NIR + GREEN)} \quad (3)$$

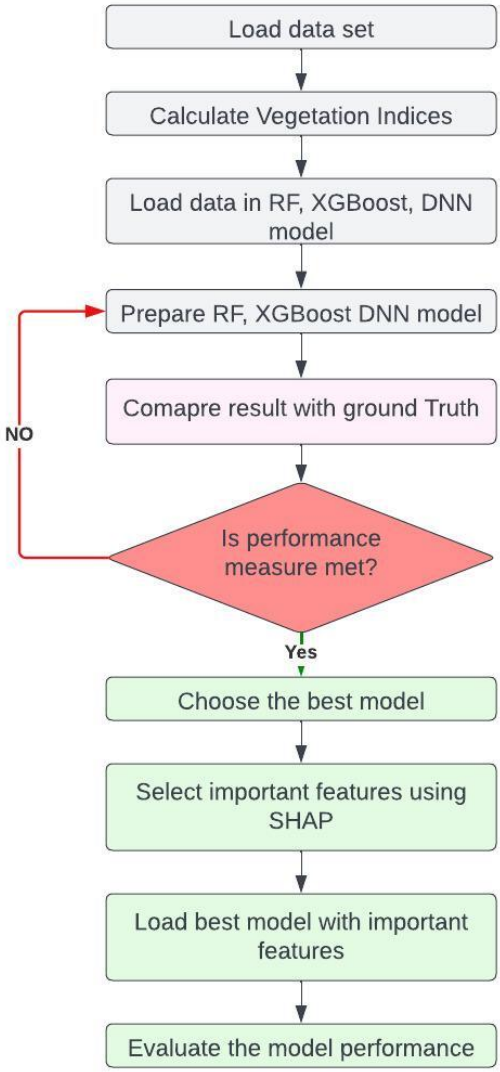

Fig. 2: The step-by-step methodology for interpretable ML and DNN models

Normalized Difference Water Index (NDWI) is generated from near-infrared (NIR) and the short-wave infrared (SWIR) bands. It reflects changes in vegetation water status [24]. In most circumstances, NDWI is used for effective water identification [25]. However, studies show that [24] this index is effective for removing the influence of vegetation structure and volume.

$$NDWI = \frac{(NIR - SWIR)}{(NIR + SWIR)} \tag{4}$$

The indices were added to the dataset as three different features. The dataset was then split randomly into training and testing sets. The next step was designing the DNN architecture using this data.

3.2 DNN Architecture

DNN architectures are widely used in land cover classification [26, 27]. A feed-forward neural network is an artificial neural network in which information flows in one direction, i.e., from the input layer to the output layer, without any feedback loops. It is a fundamental and widely used model in ML and deep learning. Each layer comprises multiple neurons, and neighbouring neurons are fully connected. The input layer accepts input data, the output layer generates the final output, and the hidden layers apply transformations to the input data using activation functions. The output of each neuron in a layer is calculated using the following equation:

$$z_i^{(k)} = \sum_{j=1}^{n^{(k-1)}} w_{ij}^{(k)} a_j^{(k-1)} + b_i^{(k)} \tag{5}$$

where $z_i^{(k)}$ is the weighted sum of the inputs to neuron i in layer k, $n^{(k-1)}$ is the number of neurons in the previous layer, $w_{ij}^{(k)}$ is the weight of the connection between neuron i in layer k and neuron j in layer $k-1$, $a_j^{(k-1)}$ is the activation of neuron j in layer $k-1$, and $b_i^{(k)}$ is the bias term of neuron i in layer k.

The output of each neuron is passed through an activation function f to introduce non-linearity, which is defined as follows:

$$a_i^{(k)} = f(z_i^{(k)}) \tag{6}$$

The activation function f can be a sigmoid, ReLU, or other function depending on the problem and network architecture. In all layers, we use ReLU as the activation function; in the output layer, we use Softmax as activation. The categorical cross-entropy (CCE) is used for the loss function [28] at compilation time, which is calculated as follows:

$$H(p, q) = -\sum_{i=1}^{C} p_i log(q_i) \tag{7}$$

where p is the true probability distribution of the classes, q is the predicted probability distribution of the classes, and C is the number of classes.

Table **??** describes the layer-by-layer architecture of our proposed DNN model. It provides information about the type of each layer, its input and output shape, and the number of parameters in the layer. This particular architecture has six layers in total, including three dense layers, 1 batch normalization layer, and two activation layers (ReLU and Softmax). The input shape of the model is nine since the input data has nine features. The output shape of the model is five since there are five classes to

Table 3: Proposed DNN Architecture

Layer No.	Layer Type	Input Size	Output Size	Number of Parameters
1	Dense (Input Layer)	(9,)	(32,)	320
2	BatchNorm	(32,)	(32,)	128
3	Dense	(32,)	(32,)	1056
4	Dense	(32,)	(32,)	1056
5	Dense	(32,)	(5,)	165
6	Dense (Output Layer)	(5,)	(5,)	30
Total Parameters				2755
Total Trainable Parameters				2691
Non-Trainable Parameters				64

predict. The total number of parameters in the model is 2,755, which is calculated as the sum of the number of parameters in each layer.
Figure 3 helps to understand the performance of our model. The training loss plot depicts the change in loss (i.e., error) during training. As the model learns from the training data, the loss should ideally decrease over time. If the loss reaches a plateau or begins to climb, it could mean that the model is overfitting the training data or that the learning rate needs to be modified. The validation loss plot depicts the change in loss on data that the model did not see during training. This graphic aids in evaluating the model's generalization performance. If the validation loss begins to rise as the training loss falls, it may signal that the model is overfitting to the training data and cannot generalize successfully to new data. In the "Model Loss" figure, the validation loss from the proposed model more or less traces the training loss curve, which signifies a stable and generalized model. The training and validation

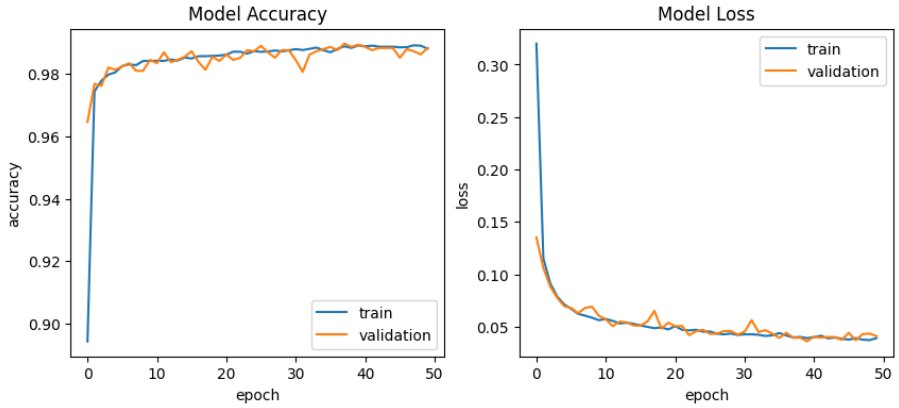

Fig. 3: DNN Training and Validation Accuracy and Loss

accuracy plot shows how classification accuracy changes throughout training. The model's accuracy should improve over time as it learns from the training data. If the accuracy on the validation set plateaus or begins to decline, it may suggest that the

model is overfitting the training data or that the learning rate needs to be changed. Our model's training and validation accuracy curves increase over time, and the validation accuracy curve more or less follows the training accuracy curve except for a few zigzags. The scale difference on the Y-axis is very small (0.02), so it can be easily ignored.

3.3 SHAP Approach

Using game theory, SHAP [29] describes the model's effectiveness. To make the method easy to comprehend, SHAP utilizes an additive feature imputation approach, where the target model is expressed as the sum of input parameters in a linear manner[30, 31]. Several methods have been proposed to account for model predictions. Previously proposed explanation techniques, such as DeepLIFT [32, 33] and LIME, are gathered in the SHAP structure [34] under the category of additive feature attribution approaches. Using Shapley values gives each variable that meets the following conditions a significance value (SHAP value), which helps explain the prediction in question.
Shapely values, named after Lloyd Shapely and denoted by $L_i(v)$, are a solution to a coalition game where there is a set of P features and a value function u that maps each subset of features to its importance. Formally, $u : 2P \rightarrow R$ with $u(\phi) = 0$ (empty set is zero). For feature i and value function u, the SHAP value is as follows:

$$L_{(i)}(u) = \frac{1}{P} \sum\nolimits_{S \subseteq P \setminus \{i\}} \left(\frac{P-1}{|S|} \right)^{-1} \left(u\left(S \cup \{i\}\right) - u\left(S\right) \right) \tag{8}$$

As this research article aims to find the top 10 features to simplify the classification process, SHAP is employed to find the important features of each classifier. Tree SHAP, Deep SHAP, and Kernel SHAP are just a few of the methods that can be used to estimate SHAP values [34]. Kernel SHAP is used in this work because it provides more accurate estimates with fewer model assessments than alternative sampling-based methods [30].

3.4 Model Implementation

To assess the impact of features on land cover, we first input all of the features into the models and receive classification results. After determining the importance of the features acquired by the SHAP approach, we entered the high-impact features into the best ML framework and secured the classification results. The most recent classification results are compared with previous research articles.

3.5 Comparison of the DNN Model with Random Forest and XGBoost

The performance of Random Forest and XGBoost is compared with the proposed deep learning model. SHAP is used to determine significant variables and their effects on classification results. A top-performing model is then fed with "n" important features to prove their importance.

3.5.1 Random Forest Classifier

Random Forest is a popular ensemble learning method in ML [35, 36]. It is based on decision trees and creates multiple trees to make a prediction. To determine which attributes to consider, the classifier uses the Gini Index, which measures the degree of impurity in an attribute compared to the available classes. Suppose there is a training set M containing many cases (pixels). When we randomly pick one case (pixel) from the set, we can assign it to a specific class called P_i, where the Gini index will be

$$\sum \sum_{i \neq j} \left(f\left(P_i, M\right)/|M|\right)\left(f\left(P_j, M\right)/|M|\right) \tag{9}$$

where $f(P_i, M)/M$ is the probability that the selected case belongs to class P_i [37]. The RF model has been tested with fivefold cross-validation and hyperparameters tuning. The hyperparameters and their respective values are listed in the table 4, which are best suited for our data set.

Table 4: Random Forest Hyperparameters and Optimum Values

Hyperparameters	**Values**
N_estimators	100
Min_samples_leaf	1
Max_depth	None
Criterion	Gini
Max_features	Sqrt
Min_samples_split	2

3.5.2 XGBoost

XGBoost is a highly used ML algorithm for land use land cover classification [38–40]. It is a gradient-boosting algorithm that enhances the accuracy and efficiency of ML models. The primary concept behind XGBoost is to iteratively train weak learners and integrate them into a powerful final learner to achieve superior prediction accuracy. Let's denote the training data set as $D = (p_1, y_1), (p_2, y_2), ..., (p_n, y_n)$, where p_i is the $i-th$ input feature vector and y_i is the corresponding target output. XGBoost aims to learn a function $F(p)$ that maps input features to output targets. The function $F(p)$ is represented as a sum of M weak learners $f(p, \theta m)$, where θm denotes the parameters of the $m-th$ weak learner, and M is the number of weak learners in the final model.

$$F(p) = \sum m = 1^M f(p, \theta m) \tag{10}$$

The weak learners are trained using a gradient-boosting algorithm. At each iteration, the algorithm tries to fit a weak learner h(p) to the negative gradient of the loss

function $L(y, F(p))$, which is given by:

$$g_i = -[\partial(L(y_i, F(p_i)))/(\partial(F(p_i)))] \tag{11}$$

The weak learner h(p) is trained to minimize the following loss function:

$$Lm = \sum i = 1^n [y_i - (Fm - 1(p_i) + hm(p_i))]^2 + \Omega(hm) \tag{12}$$

Here, $Fm - 1(p_i)$ denotes the output of the model at the $(m-1) - th$ iteration, and $\Omega(hm)$ is a regularization term that penalizes the complexity of the weak learner. The learning rate is denoted by η, and it controls the contribution of each weak learner to the final model.

Finally, the updated model at the m-th iteration is given by:

$$Fm(p_i) = Fm - 1(p_i) + \eta hm(p_i) \tag{13}$$

In summary, XGBoost is a powerful algorithm that uses gradient boosting to iteratively train weak learners and add them to a final strong learner. The algorithm is flexible, fast, and can handle various ML tasks, including classification, regression, and ranking. The XGBoost model has been tested with fivefold cross-validation and hyperparameter tuning. In the table 5, the hyperparameters and their respective values are listed, which are best suited for our data set.

Table 5: XGBoost hyperparameters and optimum values

Hyperparameter	**Values**
Max Depth	2
N estimators	60
Nthread	4
Objective	multi:softprob
Seed	42
Learning Rate	0.1

3.6 Model Evaluation Matrices

The metrics commonly used to evaluate the performance of classification models are precision, F1 score, and recall. On the other hand, overall accuracy is a metric used to evaluate the performance of both regression and classification models. [41]. Here's a concise explanation of each:

- Recall: Recall is the fraction of true positives (correctly predicted positive instances) out of all actual positive instances in the data set. It measures how well a model can identify all positive instances and avoid false negatives.

$$Recall = (\alpha)/(\alpha + \gamma) \tag{14}$$

- Precision: Precision is the fraction of true positives out of all predicted positive instances. It measures how well a model avoids false positives and correctly identifies positive instances.

$$Precision = \alpha/(\alpha + \beta) \tag{15}$$

- F1 score: F1 score is the harmonic mean of recall and precision. It combines both metrics into a single score that balances both precision and recall. The F1 score ranges from 0 to 1, with a higher score indicating better model performance.

$$F1score = 2 * \kappa * \delta/(\kappa + \delta) \tag{16}$$

- Overall Accuracy: Overall accuracy measures the proportion of correct predictions (true positives and true negatives) out of all predictions. It is commonly used in classification and regression problems and measures the model's overall performance.

$$OA = (\alpha + \mu)/N \tag{17}$$

Using Equations 14,15,16,17 all the above mentioned evaluation matrices are calculated, where

- FP = False Positive Pixels = β
- TP = True Positive Pixels = α
- FN = False Negetive Pixels = γ
- TN = True Negetive Pixels =μ
- Recall= δ
- Precision=κ

4 Results and discussions

Tables 6, 7 and 8 show the evaluation matrices for the new DNN model, RF and XGBoost models respectively, when all the bands, including the indices bands,were considered. When compared, the overall accuracy of the DNN was the highest at 98.9% followed by XGBoost with overall accuracy of 98.1% and RF with overall accuracy of 97%. In general all the models performed well in identifying the water, mangroves and others. The extent of mud flats and sand banks being less in the scene, not much data could be provided to the model. To overcome this drawback, dataset balancing techniques could be used. In this work it was not done because oversampling of data may lead to overfitting problems whereas undersampling may have resulted in loss of a good number of data points from the user data set. However, as we can observe from Table 6, the new DNN model showed no bias in these two classes and maintained a good score in the evaluation matrices.

SHAP is used to interpret ML models' results by determining each feature's significance in making the final prediction. According to Garc´ıa and Az-narte [31], a bar plot is a useful means to show the overall feature importance in a model and identify which features have the most significant influence on predictions. Figure 4(a, b, c) shows a bar plot for the three models studied in the present work. Each bar in the plot indicates a feature. The length of each bar represents the extent of influence of

Table 6: DNN Model Evaluation Matrices

	Water	Mangrove	SandBank	MudFlat	Other
F1-score	1.00	0.98	0.95	0.97	1.0
Recall	1.00	0.99	0.97	0.96	1.0
Precision	1.00	0.98	0.93	0.98	1.0
OA			**0.989**		

Table 7: RF Model Evaluation Matrices

	Water	Mangrove	SandBank	MudFlat	Other
F1-score	1.00	0.97	0.79	0.91	0.96
Recall	1.00	0.98	0.70	0.89	0.98
Precision	1.00	0.95	0.89	0.93	0.95
OA			**0.970**		

Table 8: XGBoost Model Evaluation Matrices

	Water	Mangrove	SandBank	MudFlat	Other
F1-score	1.00	0.99	0.97	0.97	0.99
Recall	1.00	0.99	0.96	0.95	1.0
Precision	1.00	0.98	0.97	0.98	0.99
OA			**0.981**		

the concerned feature on the model's output. Longer bars indicate a stronger influence on the prediction and vice versa. The positive or negative values of the bars indicate whether the feature increases the prediction or decreases. Hence, from the plot 4(a) it can be infrared that the features of Blue, NIR, Green and Red have maximum impact on the DNN model.

Another important visualization technique used in the SHAP framework is bee swarm plots. These plots represent the magnitude of the impact of the features. In a bee swarm plot, the features or individual instances are plotted as vertical dots along the y-axis. Dots along the x-axis represent SHAP values for a specific feature. This kind of plot provides insight into the relationship between feature values and the impact on predictions, showing how different instances behave. By visualizing the density of data points for each feature, we can infer which features impact the model's output most. This information is useful for feature selection, model tuning, and model interpretation. Figure 5 (a,b,c) shows bee swarm plots for each model used in the current research work. For the proposed DNN model it was observed that the density was highest for Blue, followed by NIR, Green, Red, EVI, SWIR1, NDWI, GNDI, SWIR2.

From Figures 4(a,b,c) and 5(a,b,c) it is evident that different models may prioritize different features, and feature importance rankings may differ between models. Hence, to identify the most critical features for a given problem, feature importance rankings of all the models are compared. Feature weights are calculated using Equation 18.

Here N is the number of models used, which in our case is 3, NF is the total number of features, which is nine here, and FI(i) is feature importance in the i^{th} model.

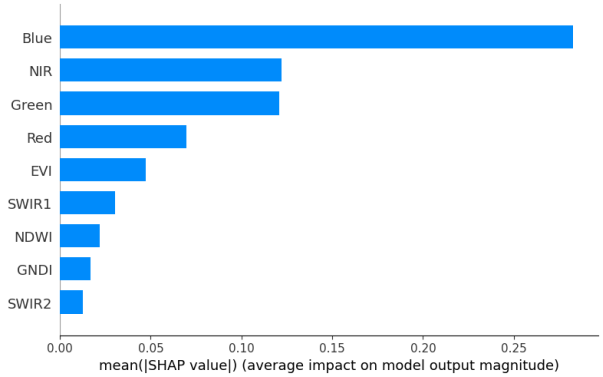

(a) Important Features of DNN Model

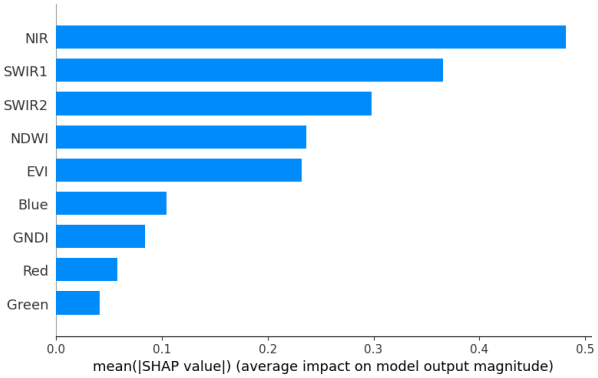

(b) Important Features of RF Model

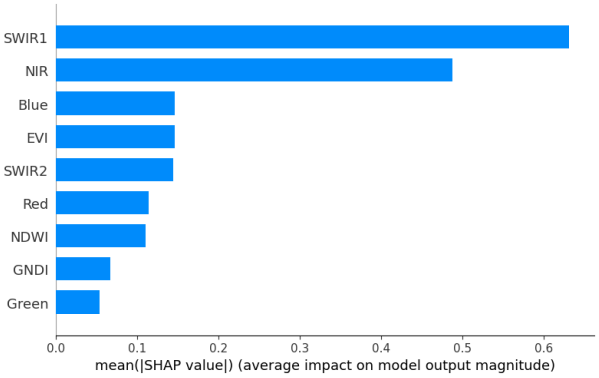

(c) Important Features of XGBoost Model

Fig. 4: SHAP Summary Plot

$$FeatureWeight = \sum_{i=1}^{N} (NF - FI_{(i)}) \tag{18}$$

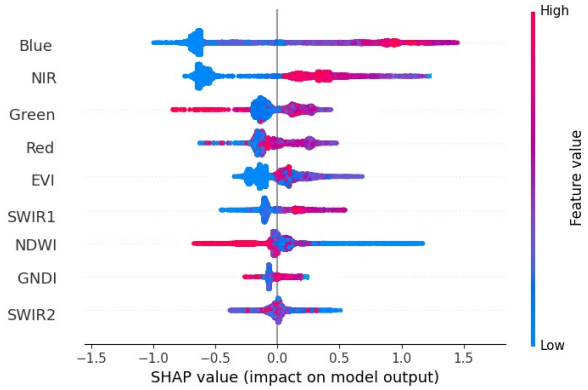

(a) Bee Swarm Plot of the DNN Model

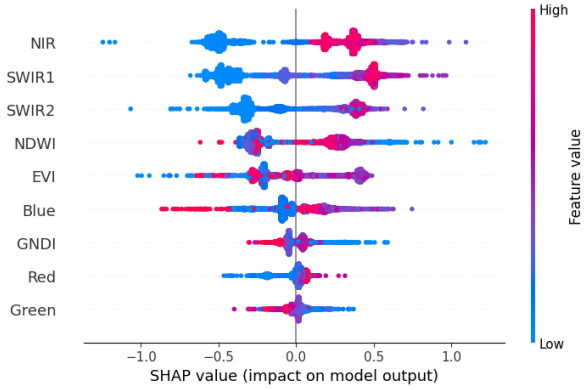

(b) Bee Swarm Plot of the RF Model

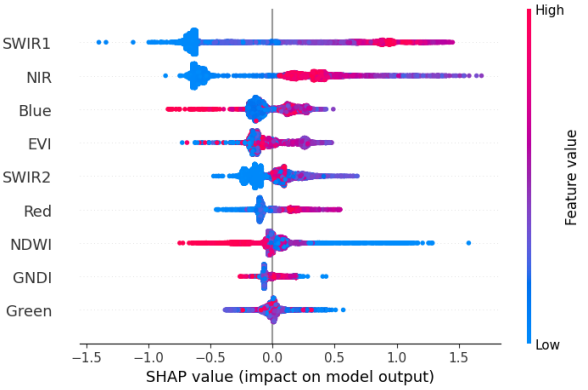

(c) Bee Swarm Plot of the XGBoost Model

Fig. 5: SHAP Bee Swarm Plot

The feature weights showed that NIR, SWIR1, Blue, and EVI are the most important features. The DNN model was then simplified by using these four important features as input hence, with fewer trainable parameters. This approach reduces the risk of overfitting and also improves the model's generalization. Table 9 describes the DNN model architecture with the four important features. Table 10 shows the model evaluation result of the simplified DNN model.

Table 9: DNN Architecture With Important Features

Layer No.	Layer Type	Input Size	Output Size	Number of Parameters
1	Dense (Input Layer)	(4,)	(32,)	160
2	BatchNorm	(32,)	(32,)	128
3	Dense	(32,)	(32,)	1056
4	Dense	(32,)	(32,)	1056
5	Dense	(32,)	(5,)	165
6	Dense (Output Layer)	(5,)	(5,)	30
Total Parameters				2595
Total Trainable Parameters				2531
Non-Trainable Parameters				64

Table 10: DNN Model Evaluation Result With Four Important Features

	Water	Mangrove	SandBank	MudFlat	Other
F1-score	1.00	0.98	0.94	0.95	0.99
Recall	1.00	0.99	0.94	0.94	0.99
Precision	1.00	0.97	0.95	0.96	0.99
OA			**0.985**		

Figure 6(a,b) shows the confusion matrices for the original and the simplified DNN Models respectively. It can be observed from the matrices that the mangrove classification significantly improved when the simplified DNN model with important features was used. However, a few erroneous classifications of the SandBank and MudFlats class were observed. This may be attributed, as already stated, to the fact that the dataset was slightly imbalanced. Figure 7(a, b) shows the classification images generated by the two DNN models respectively

Figure 6(a,b) shows the confusion matrices for the original and the simplified DNN Models respectively. It can be observed from the matrices that the mangrove classification significantly improved when the simplified DNN model with important features was used. However, a few erroneous classifications of the SandBank and MudFlats class were observed. This may be attributed, as already stated, to the fact that the dataset was slightly imbalanced. Figure 7(a, b) shows the classification images generated by the two DNN models respectively.

Table 11 presents a comparison of the present work with other recent research carried out in the same region. It is observed that the DNN model proposed in the current work

has a higher performance compared to other methods. Hence, it can be considered as an effective model for mapping land cover using remote sensing images.

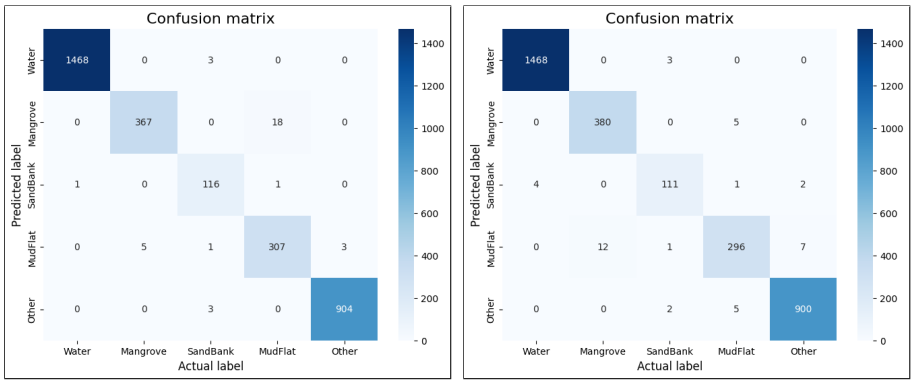

(a) Confusion Matrix of DNN Model With All Features

(b) Confusion Matrix of DNN Model DNN Model With Important Features

Fig. 6: Confusion Matrices

Table 11: Comparative Analysis With Recent Papers

Reference	Methodology	Accuracy %	Important Feature Selection	Optimization Of Model
[13]	ISODATA Maximum Likelyhood	92.33%	×	×
[16]	ISODATA	89.89%	×	×
[17]	Continuous Change Detection and Classification (CCDC)	94.5%	×	×
[18]	MLP and SVM	80.33%	×	×
[20]	Maximum Likelyhood	80.00%	×	×
[42]	Transfer learning with UNet Model	98%	×	×
[20]	Maximum Likelihood classifier	80%	×	×
[18]	Support Vector Machine MLP-Markov model	94.75%	×	×
Current paper	DNN Model	98.5%	SHAP model used	DNN Model Recompiled with important features

5 Conclusion

The study created a DNN model using reflectance from Landsat 8 images. The overall accuracy of the model was found to be higher than the RF and XGBoost models.

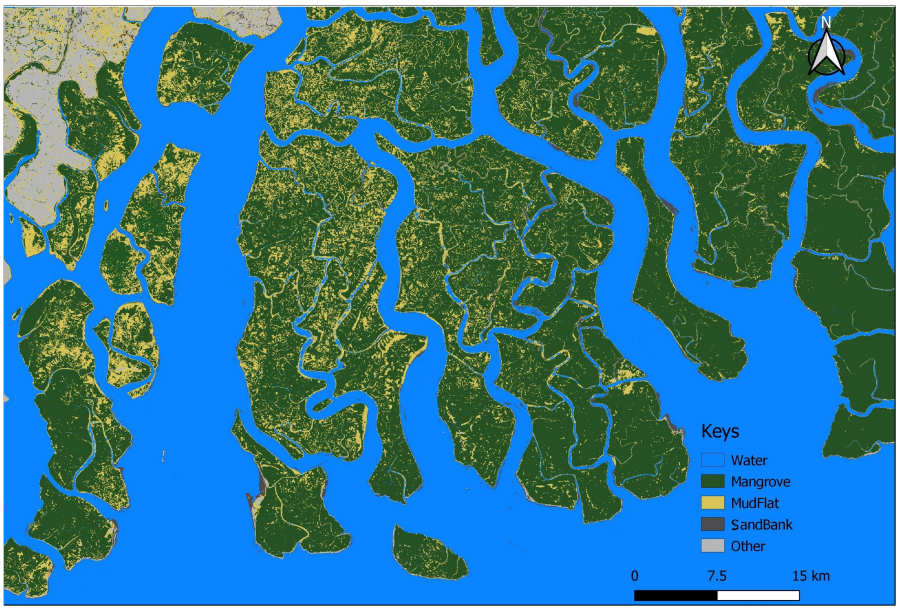

(a) Classification Image From DNN Model With All Features

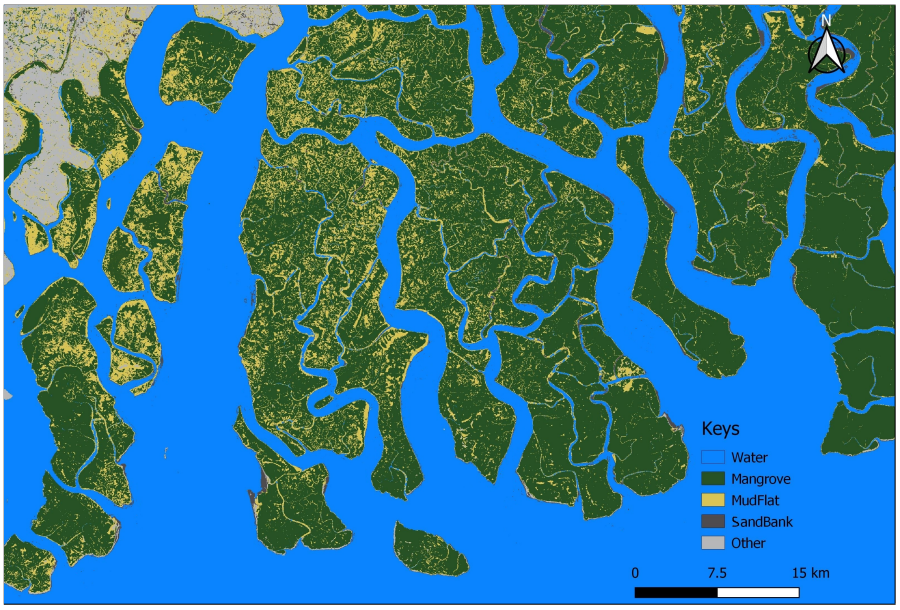

(b) Classification Image From DNN Model With Important Features

Fig. 7: Classification Images

Using the concept of explainable AI, SHAP technique was used for important feature selection. In order to make the model robust, the critical features were identified

using the insights developed from all the three models. Calculation of feature weights resulted in identification of four important features namely NIR, SWIR1, Blue, and EVI. The DNN model was then simplified. It was redesigned using only the above four features as input and hence fewer trainable parameters. However, the imbalance of the dataset resulted in a few misclassifications. In order to avoid the perils of data balancing, for the purpose of mangrove classification these misclassifications were overlooked. It is hoped that these findings can provide valuable insights for future studies in land cover classification, environmental monitoring and management using remote sensing and ML techniques. It is also believed that in the present study, some potential topics of future studies are underlain. For example,

- Researchers can attempt using other deep learning architectures, such as Convolutional Neural Networks (CNNs) or Recurrent Neural Networks (RNNs) for land cover classification.
- A comparative study on the performance of different deep learning architectures on the same data set can be done. item Though the present study achieved high accuracy on the data set used, evaluating the generalizability of the models to other data sets is important. A future study aiming to explore the performance of the models on other remote sensing data sets, such as synthetic aperture radar (SAR) or LIDAR, with different geographical regions can be undertaken.
- There is scope for further investigations of the effect of incorporating additional data sources into subsequent research works. Rather than considering data from only one satellite, multi satellite data can be incorporated to improve land cover classification accuracy

References

[1] Swetanisha, S., Panda, A.R., Behera, D.K.: Land use/land cover classification using machine learning models. International Journal of Electrical & Computer Engineering (2088-8708) **12**(2) (2022)

[2] Bayas, S., Sawant, S., Dhondge, I., Kankal, P., Joshi, A.: Land use land cover classification using different ml algorithms on sentinel-2 imagery. In: Advanced Machine Intelligence and Signal Processing, pp. 761–777. Springer, ??? (2022)

[3] Vali, A., Comai, S., Matteucci, M.: Deep learning for land use and land cover classification based on hyperspectral and multispectral earth observation data: A review. Remote Sensing **12**(15), 2495 (2020)

[4] Helber, P., Bischke, B., Dengel, A., Borth, D.: Introducing eurosat: A novel dataset and deep learning benchmark for land use and land cover classification. In: IGARSS 2018-2018 IEEE International Geoscience and Remote Sensing Symposium, pp. 204–207 (2018). IEEE

[5] Rousset, G., Despinoy, M., Schindler, K., Mangeas, M.: Assessment of deep learning techniques for land use land cover classification in southern new caledonia. Remote Sensing **13**(12), 2257 (2021)

[6] Haralick, R.M., Shapiro, L.G.: Image segmentation techniques. Computer vision, graphics, and image processing **29**(1), 100–132 (1985)

[7] Sharma, N., Aggarwal, L.M.: Automated medical image segmentation techniques. Journal of medical physics/Association of Medical Physicists of India **35**(1), 3 (2010)

[8] Kemker, R., Salvaggio, C., Kanan, C.: Algorithms for semantic segmentation of multispectral remote sensing imagery using deep learning. ISPRS journal of photogrammetry and remote sensing **145**, 60–77 (2018)

[9] Barik, D., Mondal, M.: Object identification for computer vision using image segmentation. In: 2010 2nd International Conference on Education Technology and Computer, vol. 2, pp. 2–170 (2010). IEEE

[10] Raghavan, R., Verma, D.C., Pandey, D., Anand, R., Pandey, B.K., Singh, H.: Optimized building extraction from high-resolution satellite imagery using deep learning. Multimedia Tools and Applications **81**(29), 42309–42323 (2022)

[11] Wang, Y., Gu, L., Li, X., Ren, R.: Building extraction in multitemporal high-resolution remote sensing imagery using a multifeature lstm network. IEEE Geoscience and Remote Sensing Letters **18**(9), 1645–1649 (2020)

[12] Giri, C., Ochieng, E., Tieszen, L.L., Zhu, Z., Singh, A., Loveland, T., Masek, J., Duke, N.: Status and distribution of mangrove forests of the world using earth observation satellite data. Global Ecology and Biogeography **20**(1), 154–159 (2011)

[13] Datta, D., Deb, S.: Analysis of coastal land use/land cover changes in the indian sunderbans using remotely sensed data. Geo-spatial information science **15**(4), 241–250 (2012)

[14] Sahana, M., Sajjad, H., Ahmed, R.: Assessing spatio-temporal health of forest cover using forest canopy density model and forest fragmentation approach in sundarban reserve forest, india. Modeling Earth Systems and Environment **1**(4), 1–10 (2015)

[15] Mitra, S., Basu, S.: Analysis of vegetation health of the sundarbans region using remote sensing methods. In: Proceedings of International Conference on Frontiers in Computing and Systems: COMSYS 2021, pp. 63–71 (2022). Springer

[16] Rahman, M.M., Lagomasino, D., Lee, S., Fatoyinbo, T., Ahmed, I., Kanzaki, M.: Improved assessment of mangrove forests in sundarbans east wildlife sanctuary using worldview 2 and tan dem-x high resolution imagery. Remote Sensing in Ecology and Conservation **5**(2), 136–149 (2019)

[17] Awty-Carroll, K., Bunting, P., Hardy, A., Bell, G.: Using continuous change detection and classification of landsat data to investigate long-term mangrove dynamics in the sundarbans region. Remote Sensing **11**(23), 2833 (2019)

[18] Sardar, P., Samadder, S.R.: Understanding the dynamics of landscape of greater sundarban area using multi-layer perceptron markov chain and landscape statistics approach. Ecological Indicators **121**, 106914 (2021)

[19] Nasrin, T., Ramiz, M., Sarif, M.N., Hashim, M., Siddiqui, M.A., Siddiqui, L., Mohibul, S., Mankotia, S.: Modeling of impact assessment of super cyclone amphan with machine learning algorithms in sundarban biosphere reserve, india. Natural Hazards, 1–24 (2023)

[20] Khan, A.R., Khan, A., Masud, S., Rahman, R.M.: Analyzing the land cover change and degradation in sundarbans mangrove forest using machine learning and remote sensing technique. In: Advances in Computational Intelligence: 16th International Work-Conference on Artificial Neural Networks, IWANN 2021, Virtual Event, June 16–18, 2021, Proceedings, Part II 16, pp. 429–438 (2021). Springer

[21] Sameen, M.I., Pradhan, B., Aziz, O.S.: Classification of very high resolution aerial photos using spectral-spatial convolutional neural networks. Journal of sensors **2018** (2018)

[22] Silva, V.S., Salami, G., Silva, M.I.O., Silva, E.A., Monteiro Junior, J.J., Alba, E.: Methodological evaluation of vegetation indexes in land use and land cover (lulc) classification. Geology, Ecology, and Landscapes **4**(2), 159–169 (2020)

[23] Bannari, A., Morin, D., Bonn, F., Huete, A.: A review of vegetation indices. Remote sensing reviews **13**(1-2), 95–120 (1995)

[24] Maki, M., Ishiahra, M., Tamura, M.: Estimation of leaf water status to monitor the risk of forest fires by using remotely sensed data. Remote Sensing of Environment **90**(4), 441–450 (2004)

[25] Du, Y., Zhang, Y., Ling, F., Wang, Q., Li, W., Li, X.: Water bodies' mapping from sentinel-2 imagery with modified normalized difference water index at 10-m spatial resolution produced by sharpening the swir band. Remote Sensing **8**(4), 354 (2016)

[26] Sadia, A., Uddin, S.S., Islam, R.: Transfer learning in deep neural network for land cover classification. In: 2022 25th International Conference on Computer and Information Technology (ICCIT), pp. 641–644 (2022). IEEE

[27] Rajendran, G.B., Kumarasamy, U.M., Zarro, C., Divakarachari, P.B., Ullo, S.L.: Land-use and land-cover classification using a human group-based particle swarm

optimization algorithm with an lstm classifier on hybrid pre-processing remote-sensing images. Remote Sensing **12**(24), 4135 (2020)

[28] Murugan, P.: Implementation of deep convolutional neural network in multi-class categorical image classification. arXiv preprint arXiv:1801.01397 (2018)

[29] Chen, S.: Interpretation of multi-label classification models using shapley values. arXiv preprint arXiv:2104.10505 (2021)

[30] Abdollahi, A., Pradhan, B.: Explainable artificial intelligence (xai) for interpreting the contributing factors feed into the wildfire susceptibility prediction model. Science of The Total Environment **879**, 163004 (2023)

[31] García, M.V., Aznarte, J.L.: Shapley additive explanations for no2 forecasting. Ecological Informatics **56**, 101039 (2020)

[32] Shrikumar, A., Greenside, P., Kundaje, A.: Learning important features through propagating activation differences. In: International Conference on Machine Learning, pp. 3145–3153 (2017). PMLR

[33] Kumar, C.S., Choudary, M.N.S., Bommineni, V.B., Tarun, G., Anjali, T.: Dimensionality reduction based on shap analysis: a simple and trustworthy approach. In: 2020 International Conference on Communication and Signal Processing (ICCSP), pp. 558–560 (2020). IEEE

[34] Lundberg, S.M., Lee, S.-I.: A unified approach to interpreting model predictions. Advances in neural information processing systems **30** (2017)

[35] Li, X., Chen, W., Cheng, X., Wang, L.: A comparison of machine learning algorithms for mapping of complex surface-mined and agricultural landscapes using ziyuan-3 stereo satellite imagery. Remote sensing **8**(6), 514 (2016)

[36] Jin, Y., Liu, X., Chen, Y., Liang, X.: Land-cover mapping using random forest classification and incorporating ndvi time-series and texture: A case study of central shandong. International journal of remote sensing **39**(23), 8703–8723 (2018)

[37] Pal, M.: Random forest classifier for remote sensing classification. International journal of remote sensing **26**(1), 217–222 (2005)

[38] Chemura, A., Rwasoka, D., Mutanga, O., Dube, T., Mushore, T.: The impact of land-use/land cover changes on water balance of the heterogeneous buzi sub-catchment, zimbabwe. Remote Sensing Applications: Society and Environment **18**, 100292 (2020)

[39] Saini, R., Ghosh, S.K.: Analyzing the impact of red-edge band on land use land cover classification using multispectral rapideye imagery and machine learning

techniques. Journal of Applied Remote Sensing **13**(4), 044511–044511 (2019)

[40] Abdullah, A.Y.M., Masrur, A., Adnan, M.S.G., Baky, M.A.A., Hassan, Q.K., Dewan, A.: Spatio-temporal patterns of land use/land cover change in the heterogeneous coastal region of bangladesh between 1990 and 2017. Remote Sensing **11**(7), 790 (2019)

[41] Abdollahi, A., Pradhan, B., Alamri, A.: Vnet: An end-to-end fully convolutional neural network for road extraction from high-resolution remote sensing data. IEEE Access **8**, 179424–179436 (2020)

[42] Islam, M.D., Di, L., Mia, M.R., Sithi, M.S.: Deforestation mapping of sundarbans using multi-temporal sentinel-2 data & transfer learning. In: 2022 10th International Conference on Agro-geoinformatics (Agro-Geoinformatics), pp. 1–4 (2022). IEEE